UDC 551.509.313:551.515.4:519.3

NUMERICAL VARIATIONAL ANALYSIS WITH WEAK CONSTRAINT AND APPLICATION TO SURFACE ANALYSIS OF SEVERE STORM GUST

YOSHIKAZU SASAKI

The University of Oklahoma, Norman, Okla.

ABSTRACT

An investigation of the numerical variational analysis method is made for a case of "weak constraint" where the subsidiary condition is given in the form of an approximation. The simple example of a system moving with an optimized velocity is used to illustrate the theoretical development. The method is applied to analysis of the National Severe Storms Laboratory mesonetwork data of the severe storm gust that passed over the network on May 31, 1969.

1. INTRODUCTION

In articles published previously on numerical variational analysis (Sasaki 1958, 1969*a*, 1969*b*) and in the accompanying articles (Sasaki 1970*a*, 1970*b*), dynamical constraints consistent with a numerical prediction model were used in the analysis. The author sought to satisfy these constraints exactly within a certain numerical accuracy. However, there are many phenomena for which our knowledge is insufficient to formulate rigorous dynamical and mathematical models. For example, problems associated with mesoscale phenomena are those for which empirical rules have played greater roles than rigorous dynamical and mathematical rules in understanding and forecasting the phenomena.

Suppose that a storm is moving with a translation velocity over an area where surface meteorological data are the best available. There is, to the author's knowledge, no dynamical and mathematical model that is capable of describing accurately the surface patterns and their time changes. However, translation of the patterns with a certain constant velocity in a reasonably short period has been one of the most widely used empirical rules in interpolating values between observations in time and space and in making short-range forecasts of the order of 10 min.

The numerical variational analysis method seems to offer an organized approach to such a problem. The dynamical constraints employed in the author's previous papers can be easily extended to include empirical constraints or approximate subsidiary conditions. This extension seems to be especially important for phenomena about which the dynamics is poorly understood. This article intends to demonstrate the capability of the method in handling such empirical rules as constraints and in using dynamical constraint in approximation.

2. WEAK DYNAMICAL CONSTRAINT

The dynamical constraint of the linear advection equation is assumed to be given by

$$\frac{\partial\varphi}{\partial t}+c_x\frac{\partial\varphi}{\partial x}=0 \tag{1}$$

which is written in a form of the finite-difference equation

$$\nabla_t\varphi+c_x\nabla_x\varphi=0 \tag{2}$$

where φ is a meteorological variable and c_x is the advection speed in the x direction. The finite-difference operators ∇_t and ∇_x are defined on a grid system

$$\nabla_t\varphi=\frac{\varphi_{n+1}-\varphi_{n-1}}{2\Delta t}$$

and (3)

$$\nabla_x\varphi=\frac{\varphi_{i+1}-\varphi_{i-1}}{2\Delta x}.$$

The time and space increments between consecutive points in the t–x space are denoted by Δt and Δx, respectively, and φ is assigned at all grid points. The nth time level is represented by the subscript n and ith grid point in the x direction is denoted with the subscript i. The subscripts are integers.

There are various types of formalisms in numerical variational analysis based on the constraint (2). They may be classified into three basic types (Sasaki 1970*a*).

The first formalism is written in the form

$$\delta J=\delta\sum_{n,i}\{\tilde{\alpha}(\varphi-\tilde{\varphi})^2+\alpha_t(\nabla_t\varphi)^2\}=0 \tag{4}$$

where J is a functional defined as $\Sigma\{\ \}$ and $\tilde{\alpha}$ and α_t are the weighting factors. The first term is the universal one that minimizes the difference between the observed and analyzed values, and the second is the term filtering out high-frequency modes that are unnecessary in the analyzed field. The variational eq (4) is solved with constraint (2). This formalism was discussed in detail in the author's articles (1969*a*, 1969*b*, 1970*b*).

Another formalism is orthodox and is expressed by the equation of variation

$$\delta J=\delta\sum_{n,i}\{\tilde{\alpha}(\varphi-\tilde{\varphi})^2+\lambda(\nabla_t\varphi+c_x\nabla_x\varphi)\}=0 \tag{5}$$

where λ is the Lagrange multiplier to which δ should be operated (Courant and Hilbert 1953). This formalism is discussed in Sasaki (1970*a*).

408-301 O - 70 - 4

In the above formalisms, constraint (2) should be satisfied exactly. In contrast, there are a number of cases where constraint (2) is approximately satisfied. Most of the empirical rules found for the mesoscale phenomena are of a type where unknown complicated mechanisms are playing certain roles and the empirical rules are only satisfied in an approximate sense. In this case, a better variational formalism will be

$$\delta J=\delta\sum_{n,i}\{\tilde{\alpha}(\varphi-\tilde{\varphi})^2+\alpha(\nabla_t\varphi+c_x\nabla_x\varphi)^2\}=0 \tag{6}$$

where α is a weighting factor instead of a Lagrange multiplier. The variational operator should not be applied to α. A similar formalism was proposed by Thompson (1969). One of the other differences between eq (5) and (6) is that the term $(\nabla_t\varphi+c_x\nabla_x\varphi)$ appears in linear form in eq (5) and in quadratic form in eq (6). Therefore, the Lagrange condition is always satisfied in eq (6), and the constraint is now expressed as

$$\nabla_t\varphi+c_x\nabla_x\varphi\doteq 0. \tag{7}$$

3. THE EULER EQUATION

In this article, discussion will be given only for formalism (6). Solution of eq (6) is obtained by deriving the Euler equation under the assumption that the variation $\delta\varphi$ vanishes at the boundary, that is,

$$(\delta\varphi)_B=0. \tag{8}$$

In the derivation, the commutation formula

$$\Sigma\xi\nabla\eta=-\Sigma\eta\nabla\xi \tag{9}$$

of the finite-difference analog is used. The ξ and η are arbitrary variables, ∇ represents ∇_t or ∇_x, and Σ is the sum of the variable over the entire grid points. The proof of eq (9) is given in Sasaki (1969*b*).

The Euler equation for eq (6) becomes

$$\tilde{\alpha}(\varphi-\tilde{\varphi})-\alpha(\nabla_t+c_x\nabla_x)(\nabla_t\varphi+c_x\nabla_x\varphi)=0.$$

This equation is rewritten in convenient form

$$\tilde{\alpha}(\varphi-\tilde{\varphi})-\alpha\nabla_t\nabla_t\varphi-2\alpha c_x\nabla_t\nabla_x\varphi-\alpha c_x^2\nabla_x\nabla_x\varphi=0. \tag{10}$$

If Δt and Δx approach zero, eq (10) becomes a partial differential equation of the second order. On the basis of the theory of characteristics, eq (10) is a parabolic type. However, it is easier to work with the elliptic type in the actual application of this method. The type of equation can be changed by adding the terms of the low-pass filter $\alpha_t(\nabla_t\varphi)^2$ as a frequency filter and $\alpha_s(\nabla_x\varphi)^2$ as a wave number filter to eq (6);

$$\delta J=\delta\sum_{n,i}\{\tilde{\alpha}(\varphi-\tilde{\varphi})^2+\alpha(\nabla_t\varphi+c_x\nabla_x\varphi)^2 +\alpha_t(\nabla_t\varphi)^2+\alpha_s(\nabla_x\varphi)^2\}=0 \tag{11}$$

where α_t and α_s are predetermined weights. The Euler equation of eq (11) thus becomes

$$\tilde{\alpha}(\varphi-\tilde{\varphi})-(\alpha+\alpha_t)\nabla_t\nabla_t\varphi-2\alpha c_x\nabla_t\nabla_x\varphi-(\alpha+\alpha_s)c_x^2\nabla_x\nabla_x\varphi=0, \tag{12}$$

and it is an elliptic equation at the limit $\Delta t\to 0$ and $\Delta x\to 0$ since

$$\alpha^2c_x^2-(\alpha+\alpha_t)(\alpha+\alpha_s)c_x^2<0 \tag{13}$$

if α_t and/or α_s are nonzero positive (Courant and Hilbert 1962). From a practical viewpoint, the elliptic type is desirable for problems of map analysis. However, the parabolic type obtained by taking $\alpha_t=0$ and $\alpha_s=0$ may be used better for the problem of optimized prediction. Since this article only discusses the analysis problems, we assume that $\alpha_t\neq 0$ and $\alpha_s\neq 0$, although α_t and α_s may be infinitesimal.

4. LOW-PASS FILTER CHARACTERISTICS

The characteristics of the low-pass filter are discussed for the Euler eq (12). This is similar to those of Sasaki (1970*a*, 1970*b*). Suppose that the observed and analyzed fields are represented by a simple harmonic function such as

$$\begin{pmatrix}\tilde{\varphi}\\ \varphi\end{pmatrix}=\begin{pmatrix}\tilde{\Phi}\\ \Phi\end{pmatrix}e^{ikx+i\nu t} \tag{14}$$

where k is the wave number, ν is the frequency, and $\tilde{\Phi}$ and Φ are the amplitudes. The ratio $r\equiv\Phi/\tilde{\Phi}$, which is an index of the filtering response, is obtained by substitution of eq (14) into eq (12) as follows:

$$r\equiv\frac{\Phi}{\tilde{\Phi}}=\frac{\tilde{\alpha}}{\tilde{\alpha}+(\alpha+\alpha_t)\epsilon_t^2+2\alpha c_x\epsilon_t\epsilon_x+(\alpha+\alpha_s)c_x^2\epsilon_x^2} \tag{15}$$

where

$$\epsilon_t=\frac{\sin\nu\Delta t}{\Delta t}\text{ and }\epsilon_x=\frac{\sin k\Delta x}{\Delta x}. \tag{16}$$

At the limit $\Delta t\to 0$ and $\Delta x\to 0$,

$$r=\frac{\alpha}{\tilde{\alpha}+\alpha(\nu+kc_x)^2+\alpha_t\nu^2+\alpha_s(kc_x)^2}. \tag{17}$$

This result indicates that monotonic damping occurs as the frequency ν and the wave number k increase. This is a favorable characteristic of variational formalism with weak constraint. Also, it is interesting to note that the α terms of the weak constraint play a role similar to the α_t and α_s terms of the low-pass filter. In other words, even if $\alpha_t=0$ and $\alpha_s=0$, the result of filtering high frequencies and high wave numbers will be obtained by the α term alone.

The above favorable result obtained in the limited case where $\Delta t\to 0$ and $\Delta x\to 0$ is impaired if Δt and Δx are finite. Due to the behavior of ϵ_t and ϵ_x as functions of ν and k, r increases as ν approaches the frequency ν_m which is defined by $\nu_m=\pi/\Delta t$, or 2π times the Nyquist frequency. Similarly, k approaches k_m ($\equiv\pi/\Delta x$) as seen from eq (15). Also, r decreases monotonically for

$$0<\nu<\frac{\nu_m}{2}\text{ or }<k<\frac{k_m}{2}, \tag{18}$$

and r increases monotonically for

$$\frac{\nu_m}{2}<\nu<\nu_m \text{ or } \frac{k_m}{2}<k<k_m. \tag{19}$$

The condition expressed by eq (18) is desirable but that shown by eq (19) is not. The unfavorable characteristic (19) can be avoided by smoothing the field of observed values. Then an iterative procedure is applied to solve eq (12). The iterative procedure will be discussed in the next section. Since an iterative method requires the condition that the matrix $|G|\leq 1$ for all values of ν and k, the analyzed field will not amplify the small noises of high frequencies and high wave numbers in the smoothed observed field. The initial smoothing of the observed field may be accomplished by applying the so-called "Hanning" or "Hamming" filter (Blackman and Tukey 1958) one or more times. The Hanning filter, for instance, is defined in the x and t directions, respectively, as

$$\begin{aligned}\overline{(\quad)}^{x}&=[(\quad)_{i+1}+(\quad)_{i-1}+2(\quad)_i]/4\\ \text{and}\qquad&\qquad(20)\\ \overline{(\quad)}^{t}&=[(\quad)_{n+1}+(\quad)_{n-1}+2(\quad)_n]/4.\end{aligned}$$

The spectral representation of this filter is $(1+\cos k\Delta x)/2$ for the wave number space and $(1+\cos \nu\Delta t)/2$ for the frequency space. These filtering responses show suppression of amplitudes in the neighborhood of ν_m and k_m.

5. RESIDUAL EQUATION

The solution of eq (12) may be obtained by a relaxation method as a boundary value problem. The boundary conditions necessary for eq (12) are the values of φ at a closed boundary of domain considered on a t–x plane. The necessary boundary conditions are assumed to be specified. Subsitution of the νth guess $\varphi^{(\nu)}$ for φ in eq (12) gives a residual equation

$$\begin{aligned}\tilde{\alpha}\Delta\varphi^{(\nu)}-(\alpha+\alpha_t)\nabla_t\nabla_t\Delta\varphi^{(\nu)}-2\alpha c_x\nabla_t\nabla_x\Delta\varphi^{(\nu)}\\ -(\alpha+\alpha_s)c_x^2\nabla_x\nabla_x\Delta\varphi^{(\nu)}=R^{(\nu)}.\end{aligned} \tag{21}$$

The Richardson relaxation method is used to make the $(\nu+1)$th guess

$$\Delta\varphi^{(\nu+1)}=\Delta\varphi^{(\nu)}-\frac{R^{(\nu)}}{\left[\tilde{\alpha}+(\alpha+\alpha_t)\dfrac{2}{(2\Delta t)^2}+(\alpha+\alpha_s)c_x^2\dfrac{2}{(2\Delta s)^2}\right]}. \tag{22}$$

Elimination of $R^{(\nu)}$ from these two equations leads to

$$\begin{aligned}\left[\tilde{\alpha}+(\alpha+\alpha_t)\frac{2}{(2\Delta t)^2}+(\alpha+\alpha)_s c_x^2\frac{2}{(2\Delta s)^2}\right]\Delta\varphi^{(\nu+1)}\\ -\left[(\alpha+\alpha_t)\left(\nabla_t\nabla_t+\frac{2}{(2\Delta t)^2}\right)+2\alpha c_x\nabla_t\nabla_x\right.\\ \left.+(\alpha+\alpha_s)c_x^2\left(\nabla_x\nabla_x+\frac{2}{(2\Delta s)^2}\right)\right]\Delta\varphi^{(\nu)}=0\end{aligned} \tag{23}$$

The eigenvalue of the amplification matrix **G** defined as

$$\Delta\varphi^{(\nu+1)}=G\Delta\varphi^{(\nu)} \tag{24}$$

is obtained easily in this case. If $\Delta\varphi^{(\nu)}$ is expressed by a simple harmonic $e^{ikx+i\nu t}$, the operators ∇_{tt}, ∇_{tx}, and ∇_{xx} in eq (23) are substituted for by the constants, $-\sin^2\nu\Delta t/\Delta t^2$, $-\sin\nu\Delta t\sin k\Delta x/\Delta t\,\Delta x$, and $-\sin^2 k\Delta x/\Delta x^2$, respectively. Therefore, G is given by

$$G=\frac{\left[\dfrac{\alpha+\alpha_t}{2\Delta t^2}(1-2\sin^2\nu\Delta t)-\dfrac{2\alpha c_x}{\Delta t\Delta x}\sin\nu\Delta t\sin k\Delta x-\dfrac{\alpha+\alpha_s}{2\Delta x^2}(1-2\sin^2 k\Delta x)\right]}{\tilde{\alpha}+\dfrac{\alpha+\alpha_t}{2\Delta t^2}+\dfrac{(\alpha+\alpha_s)c_x^2}{2\Delta x^2}}. \tag{25}$$

The solution will converge, that is,

$$\lim_{\nu\to\infty}\{\Delta\varphi^{(\nu)},\ R^{(\nu)}\}\to 0, \tag{26}$$

when

$$G\leq 1. \tag{27}$$

This condition will occur if

$$\tilde{\alpha}\geq\frac{2\alpha c_x}{\Delta t\Delta x}. \tag{28}$$

6. AUXILIARY TERM OF CONVERGENCE

The criterion (28) will not be satisfied in areas lacking observation where the weight of the observation $\tilde{\alpha}$ is normally taken to be zero. Hence, eq (28) becomes unsatisfied. To avoid this difficulty, one adds an auxiliary term $\tilde{\alpha}_a(\varphi-\varphi_a)^2$ to the functional in eq (11) under the conditions

$$\begin{aligned}\tilde{\alpha}_a&=0\ \ldots\ \text{if } \tilde{\alpha}\neq 0\\ \text{and}\qquad&\qquad(29)\\ \tilde{\alpha}_a&=C\ \ldots\ \text{if } \tilde{\alpha}=0\end{aligned}$$

where $\tilde{\varphi}_a$ is an interpolation of neighboring $\tilde{\varphi}$ values and C is a constant larger than $2\alpha\ c_x/\Delta t\Delta x$. When adding this new term, the variational equation is written as

$$\begin{aligned}\delta J=\delta\sum_{n,i}\{\tilde{\alpha}(\varphi-\tilde{\varphi})^2+\tilde{\alpha}_a(\varphi-\tilde{\varphi}_a)^2+\alpha(\nabla_t\varphi+c_x\nabla_x\varphi)^2\\ +\alpha_t(\nabla_t\varphi)^2+\alpha_s(\nabla_x\varphi)^2\}=0.\end{aligned} \tag{30}$$

The Euler equation of (30) is

$$\begin{aligned}\tilde{\alpha}(\varphi-\tilde{\varphi})+\tilde{\alpha}_a(\varphi-\varphi_a)-(\alpha+\alpha_t)\nabla_t\nabla_t\varphi-2\alpha c_x\nabla_t\nabla_x\varphi\\ -(\alpha+\alpha_s)c_x^2\nabla_x\nabla_x\varphi=0.\end{aligned} \tag{31}$$

By adding the auxiliary term, the type of equation at the limit $\Delta t\to 0$ and $\Delta x\to 0$ is not altered, and the low-pass filter characteristics remain the same. The convergence is now given by:

$$\begin{aligned}\text{if } \tilde{\alpha}\neq 0\qquad&\tilde{\alpha}\geq\frac{2\alpha c_x}{\Delta t\Delta x},\ \tilde{\alpha}_a=0\\ \text{and}\qquad&\qquad(32)\\ \text{if } \tilde{\alpha}=0\qquad&\tilde{\alpha}_a\geq\frac{2\alpha c_x}{\Delta t\Delta x}.\end{aligned}$$

In practice, $\tilde{\alpha}_a$ is taken to be the same value as $\tilde{\alpha}$. The value of $\tilde{\varphi}_a$ is obtained by averaging the surrounding four grid-point values (in the t–x plane, six-point average on t–x,y space) of $\tilde{\varphi}$ and/or $\tilde{\varphi}_a$, if $\tilde{\varphi}_a$ is already calculated and averageable. The above averaging procedure is

repeated until all the grid points are filled with $\tilde{\varphi}$ or $\tilde{\varphi}_a$. The boundary values are obtained in the same way. The value of an observation point $\tilde{\varphi}$ is not changed by this procedure. This simple procedure is used in this study, although a more sophisticated procedure could produce better results.

7. INTERACTION

This section deals with the interaction between φ and c_x. In previous sections, c_x was assumed to be predetermined, and the solution was sought for φ only. In this section, simultaneous solutions for φ and c_x will be investigated. For simplicity, we shall assume that observations of $\tilde{\varphi}$ and $\tilde{c}_x$ are available at all grid points. This assumption allows us to drop the $\tilde{\alpha}_a$ term from eq (30). A variational formalism for the simultaneous solution may be obtained by an extension of eq (30) or eq (14) to include reasonable constraints of c_x; thus

$$\delta J=\delta \sum_{n,i} \{\tilde{\alpha}(\varphi-\tilde{\varphi})^2+\alpha(\nabla_t\varphi+c_x\nabla_x\varphi)^2 +\alpha_t(\nabla_t\varphi)^2+\alpha_s(\nabla_x\varphi)^2+\tilde{\beta}(c_x-\tilde{c}_x)^2 +\beta_t(\nabla_t c_x)^2+\beta_s(\nabla_x c_x)^2\}=0. \quad (33)$$

All terms other than $\tilde{\beta}$, β_t, and β_s have been explained. The $\tilde{\beta}$ term is the universal constraint used to minimize the difference between observed and analyzed fields. The β_t and β_s terms play the same roles as the α_t and $\tilde{\alpha}_s$ terms. The c_x equation becomes an elliptic type if β_t or β_s does not vanish at the limit $\Delta t\to 0$; the equation also filters out unnecessary high-frequency oscillations and short waves from the analyzed field.

In this case, c_x is assumed to vary with time and space just as φ is. Therefore, the Euler equations should be derived by taking the variability of φ and c_x into consideration. The Euler equations for eq (33) are

$$\tilde{\alpha}(\varphi-\tilde{\varphi})-\alpha(\nabla_t+\nabla_x\cdot c_x)(\nabla_t+c_x\nabla_x)\varphi -\alpha_t\nabla_t\nabla_t\varphi-\alpha_s\nabla_x\nabla_x\varphi=0 \quad (34)$$

and

$$\tilde{\beta}(c_x-\tilde{c}_x)-\alpha\nabla_x\varphi.\ (\nabla_t+c_x\nabla_x)\varphi-\beta_t\nabla_t\nabla_t c_x-\beta_s\nabla_x\nabla_x c_x=0. \quad (35)$$

Equations (34) and (35) are a set of simultaneous nonlinear equations. It is difficult to inspect their characteristics without using a numerical method. For convenience, a technique of small parameter expansion is employed to reveal the interaction characteristics under certain limited conditions. Let us assume that the amplitudes of $\tilde{\varphi}$, φ, $\tilde{c}_x$, and c_x are small compared with their locally constant values $\bar{\bar{\varphi}}$, $\bar{\varphi}$, $\bar{\bar{c}}_x$, and $\bar{c}_x$ and that they can be expanded as

$$\begin{aligned}\tilde{\varphi}&=\bar{\bar{\varphi}}+\epsilon\varphi',\\ \varphi&=\bar{\varphi}+\epsilon\varphi',\\ \tilde{c}_x&=\bar{\bar{c}}_x+\epsilon\tilde{c}_x',\\ c_x&=\bar{c}_x+\epsilon c_x'\end{aligned} \quad \text{and} \quad (36)$$

where $\bar{\bar{\varphi}}$, $\bar{\varphi}$, $\bar{\bar{c}}_x$, and $\bar{c}_x$ are locally constant; $\tilde{\varphi}'$, φ', $\tilde{c}_x'$, and c_x' are functions of both time and space and are of the order of 1; and ϵ is a nondimensional small parameter that is less than 1. In this article, "locally constant" means that their derivatives are neglected in differential or difference equations. Also, we assume

$$\bar{\bar{\varphi}}=\bar{\varphi} \text{ and } \bar{\bar{c}}_x=\bar{c}_x. \quad (37)$$

Linearized equations can be obtained by substituting eq (36) and (37) into eq (34) and (35) and neglecting the $0(\epsilon^2)$ terms if ϵ is sufficiently small. Thus the Euler equations of the order of ϵ are

$$\tilde{\alpha}(\varphi'-\tilde{\varphi}')-(\alpha+\alpha_t)\nabla_t\nabla_t\varphi'-2\alpha\bar{c}_x\nabla_t\nabla_x\varphi'-(\alpha+\alpha_s) \times\bar{c}_x^2\nabla_x\nabla_x\varphi'=0 \quad (38)$$

and

$$\tilde{\beta}(c_x'-\tilde{c}_x')-\beta_t\nabla_t\nabla_t c_x'-\beta_s\nabla_x\nabla_x c_x'=0. \quad (39)$$

These equations demonstrate the following important results: eq (38) is the same as eq (12) and (31) since $\tilde{\alpha}_a=0$, that is, eq (12) and (31) can be used for the cases where a certain interaction between φ and c_x exists; c_x for eq (12) and (31) can be a very smooth value, at least a locally constant value; c_x can be determined independently from φ. Of course, the above conclusions are applicable only if ϵ is sufficiently small. In general, ϵ may not be small. However, they are useful conclusions to simplify the analysis problem. From the above discussion, the importance of the β_t and β_s terms is apparent. These terms will be included in the subsequent discussion. Now, we return to the nonlinear Euler eq (34) and (35). If β_t and β_s are nonzero values, although they may be small, these nonlinear equations can be solved as a boundary value problem (appendix).

8. EXTENSION TO TWO DIMENSIONS

Consider that organized atmospheric systems are moving in an area with variable velocities and intensities. Let the velocity components be denoted as c_x and c_y in the x and y directions, respectively. The approximate equation

$$\frac{\partial\varphi}{\partial t}+c_x\frac{\partial\varphi}{\partial x}+c_y\frac{\partial\varphi}{\partial y}\doteq 0 \quad (40)$$

should be satisfied. A finite-difference form of eq (40) is written as

$$\nabla_t\varphi+c_x\nabla_x\varphi+c_y\nabla_y\varphi\doteq 0 \quad (41)$$

where the finite-difference formulation defined in eq (3) is applied to ∇_t, ∇_x, and ∇_y. The variables φ, c_x, and c_y are assumed to be assigned at all grid points; n is the nth time level with time increment Δt; i is the ith grid point that increases as x increases; j is the jth grid point number that decreases as y increases; and the variables are functions of n, i, and j. Naturally, n, i, and j are integers.

Assuming that c_x and c_y are determined independently of φ, we can write the variational equation as a two-

dimensional version of eq (33) as

$$\delta J=\delta\sum_{n,i,j}\{\tilde{\alpha}(\varphi-\tilde{\varphi})^2+\alpha_s(\varphi-\tilde{\varphi}_a)^2+\alpha(\nabla_t\varphi+c_x\nabla_x\varphi+c_y\nabla_y\varphi)^2 +\alpha_t(\nabla_t\varphi)^2+\alpha_s[(\nabla_x\varphi)^2+(\nabla_y\varphi)^2]\}=0 \quad (42)$$

and the Euler equation of (42) as

$$\tilde{\alpha}(\varphi-\tilde{\varphi})+\alpha_s(\varphi-\tilde{\varphi}_a)-\alpha(\nabla_t+\nabla_x\cdot c_x+\nabla_y\cdot c_y)\Delta\varphi -\alpha_t\nabla_t\nabla_t\varphi-\alpha_s(\nabla_x\nabla_x\varphi+\nabla_y\nabla_y\varphi)=0 \quad (43)$$

where

$$\Delta\varphi\equiv\nabla_t\varphi+c_x\nabla_x\varphi+c_y\nabla_y\varphi. \quad (44)$$

As discussed in section 7, c_x and c_y can be analyzed separately from the φ analysis. The values of c_x and c_y may be estimated from various data sources. One is, naturally, surface network data, and the other is an estimation of $\tilde{c}_x$ and $\tilde{c}_y$ from the velocity of the movement of radar echoes. The latter is a direct way to measure the velocity of movement, $\tilde{c}_x$ and $\tilde{c}_y$. The surface network data can also be a source of direct determination of the translation velocity if an isolated system passes over at least two surface stations within a reasonably short period.

If a system is not isolated but extends in one direction such as a front, we will define the translation velocity as a velocity normal to the front. If a system is not well-defined, neither isolated thunderstormlike nor frontlike, we may use the observed wind components $\tilde{u}$ and $\tilde{v}$ as $\tilde{c}_x$ and $\tilde{c}_y$, respectively. A simple method of determination of c_x and c_y from $\tilde{c}_x$ and $\tilde{c}_y$ will be used.

The variational formalism taken for c_x and c_y is

$$\delta J_c=\delta\sum_{n,i,j}\{\tilde{\beta}[(c_x-\tilde{c}_x)^2+(c_y-\tilde{c}_y)^2]+\beta_t[(\nabla_t c_x)^2+(\nabla_t c_y)^2] +\beta_s[(\nabla_x c_x)^2+(\nabla_y c_x)^2+(\nabla_x c_y)^2+(\nabla_y c_y)^2]=0. \quad (45)$$

The Euler equations for (45) are

$$\tilde{\beta}(c_x-\tilde{c}_x)-\beta_t\nabla_t\nabla_t c_x-\beta_s(\nabla_x\nabla_x+\nabla_y\nabla_y)c_x=0 \quad (46)$$

and

$$\tilde{\beta}(c_y-\tilde{c}_y)-\beta_t\nabla_t\nabla_t c_y-\beta_s(\nabla_x\nabla_x+\nabla_y\nabla_y)c_y=0. \quad (47)$$

The analysis of mesonetwork data of severe storms is performed in two steps: (1) the determination of c_x and c_y from eq (46) and (47) and (2) the determination of the φ pattern by using the values from eq (43).

9. APPLICATION TO THE SEVERE STORM GUST ANALYSIS OF MAY 31, 1969

A well-defined gust with peak wind speed of about 70 kt swept over the central Oklahoma area in the late evening of May 31, 1969. This gust was produced by severe storm systems that were moving in a northeasterly direction passing over the area about 100 mi west of Oklahoma City at about 2300 CST. Figure 1 shows a series of the evolution of severe storm echo patterns revealed by the WSR-57 radar located at the NSSL (National Severe Storms Laboratory), ESSA, Norman, Okla. The photographs shown in this figure were taken every half hour for the 2-hr period between 2200 through 2400 CST. Range marks are every 20 mi. The rectangular area ABCD is the area covered by the analysis of wind fields shown in subsequent figures. At 2200 CST, there was a line of well-developed severe storm systems (marked by I in fig. 1) that seemed to start decaying at the time. To the southwest of this line of echos, there were two echo systems (marked by II_a and II_b in fig. 1) that were near each other. They were moving to the northeast with faster speeds than echo systems I. About 2230 CST, the echo systems II amalgamated with I and grew more intense while the echo systems I continued to decay as seen from the echo patterns at 2300–2330 CST. The southern portion of the echo system entered area ABCD about 2330 CST. This produced the gust of present interest. A marked feature of that portion after 2300 CST is a sharper edge of reflectivity at the east side. The echo at the side nearest the radar is unusually clear. It is unlikely that the effect of attenuation can explain this clarity.

Three-hour synoptic surface pressure patterns from 0000 to 0900 GMT are shown in figure 2. A relatively weak cold front associated with the Low located to the west of the Great Lakes was moving southeastward. Located to the south of the front, near Lawton, Okla., was a weak, nearly stationary low-pressure center with the central pressure of 996 mb at 0000 GMT. About 6 hr later, the low-pressure center amalgamated with the southeastward-moving cold front and then, weakening slightly, moved together with the front. The severe storm system that was responsible for producing the gust of our present interest seems to have developed between 0300 and 0600 GMT near the area west of ABCD in figure 2. The three-dimensional subsynoptic conditions associated with the development of the severe storm system is of interest, and an investigation of numerical variational analysis in t, x, y, z space for the severe storm system development of this case is in progress. The discussion of subsynoptic conditions will await completion of this analysis.

Figure 3 shows an isochrone analysis of the leading edge of the gust front passage over the network stations and that of the passage time of the first peak of wind speed. The echo pattern at 2310 CST is also shown in the figure. The isochrones seem to reflect the amalgamated double structure of systems II_a and II_b.

The square area indicated by ABCD that covers all of the NSSL mesonetwork stations is also used for the domain of the analysis. A 16 × 16 grid is placed on ABCD as shown in figure 4. The grid distance is 2.5 mi. The wind data obtained from all stations for the 1-hr period 2300 through 2400 CST are analyzed simultaneously so that an analyzed pattern reflects the influences from all stations and the entire 1-hr variations. The total number of time levels used is 25, and the time increment is 2.5 min. Input wind data, direction and speed, is a 5-min running average of every minute reading from the cup anemometer wind traces. The data were supplied by the NSSL. The value at 2302.5 is obtained, for instance, by taking the simple arithmetic average of the two adjacent readings 2302 and 2303. The data at 2305 CST are the data of direct

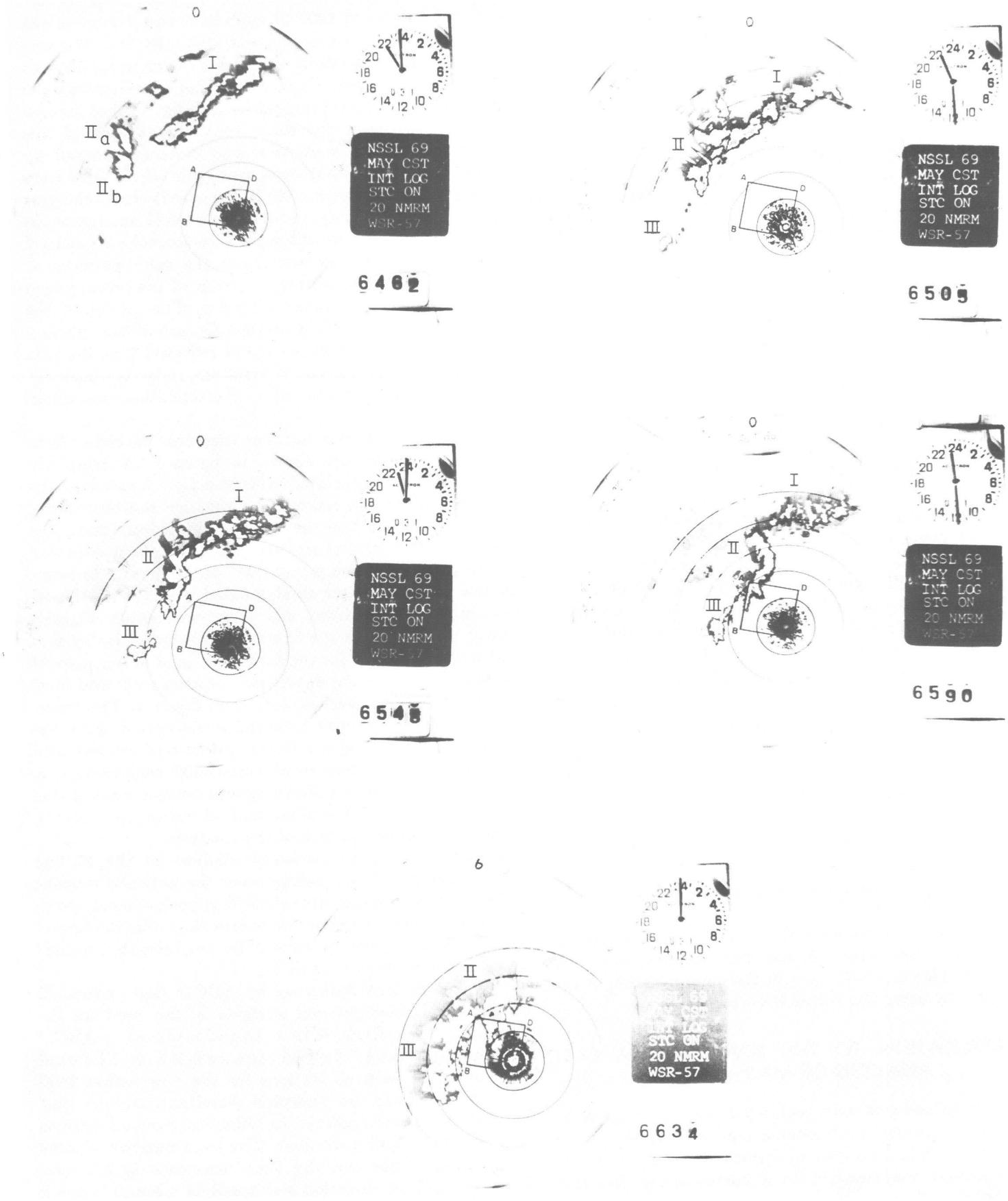

FIGURE 1.—Evolution of echo patterns as observed on the WSR–57 radarscope at the NSSL at Norman, Okla. ABCD represents the area of analysis.

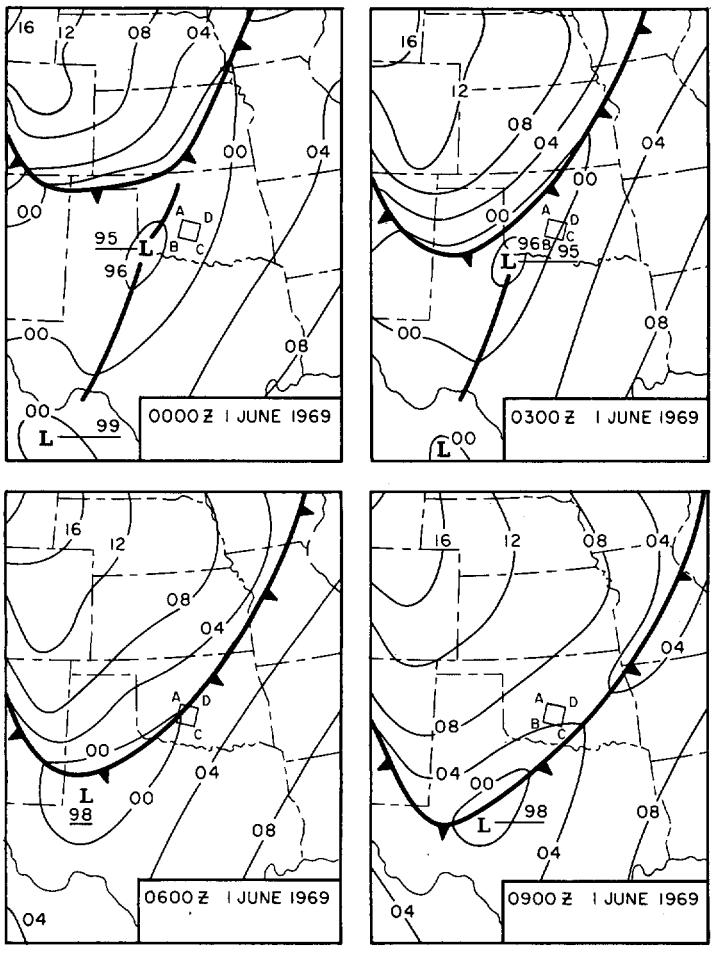

FIGURE 2.—Surface isobar patterns. Storms developed between 0300 and 0600 GMT in the vicinity of the analysis area ABCD.

reading. By using this procedure with the aid of a computer, data samples were obtained for the analysis at 2302.5, 2305, 2307.5, 2310, . . . , 2400 CST for all stations.

The estimate of $\tilde{c}_x$ and $\tilde{c}_y$ is made from the isochrone analysis (fig. 4). The normal component $\tilde{c}_n$ of the velocity of the gust front movement is calculated at various points in ABCD from the positions of the front at two successive times along the direction normal to the front. Components $\tilde{c}_x$ and $\tilde{c}_y$ are calculated by taking x and y components of $\tilde{c}_n$. These data are used to obtain c_x and c_y after substituting $\tilde{c}_x$ and $\tilde{c}_y$ into eq (46) and (47). Since the gust was a well-defined organized line that was not moving with the surface wind at the location of the front, only $\tilde{c}_x$ and $\tilde{c}_y$ are used, and the observed wind velocity components $\tilde{u}$ and $\tilde{v}$ are not used to estimate c_x and c_y. The choice of proper weight values was made by nondimensionalizing the weights;

$$\tilde{\beta}'=\tilde{\beta}/c^{*2},\ \beta_t'=\beta_t\Delta t^2/c^{*2},$$

and

$$\beta_s^2=\beta_s\Delta s^2/c^{*2}$$

where c^* is the characteristic speed (10 kt) of the front movement. The $\tilde{\beta}'$, β_t', and β_s' are taken to be equal in the calculation.

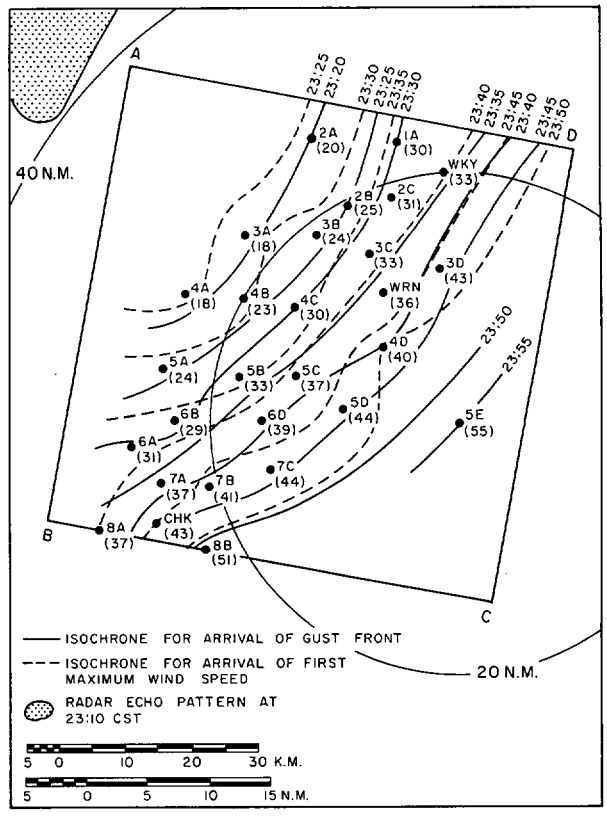

FIGURE 3.—Isochrone patterns of arrival times of the leading edge of the gust and the first maximum wind speed.

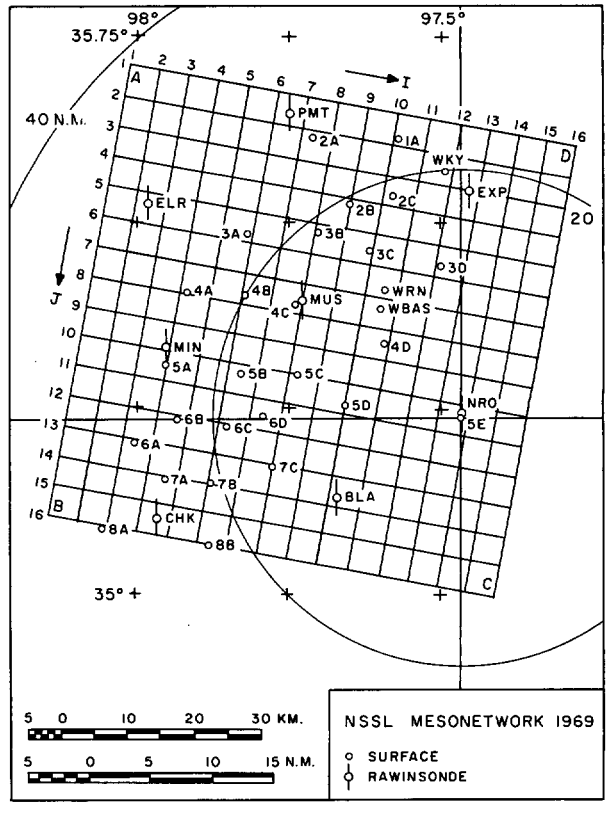

FIGURE 4.—NSSL mesonetwork stations in 1969 and the grid used for the analysis.

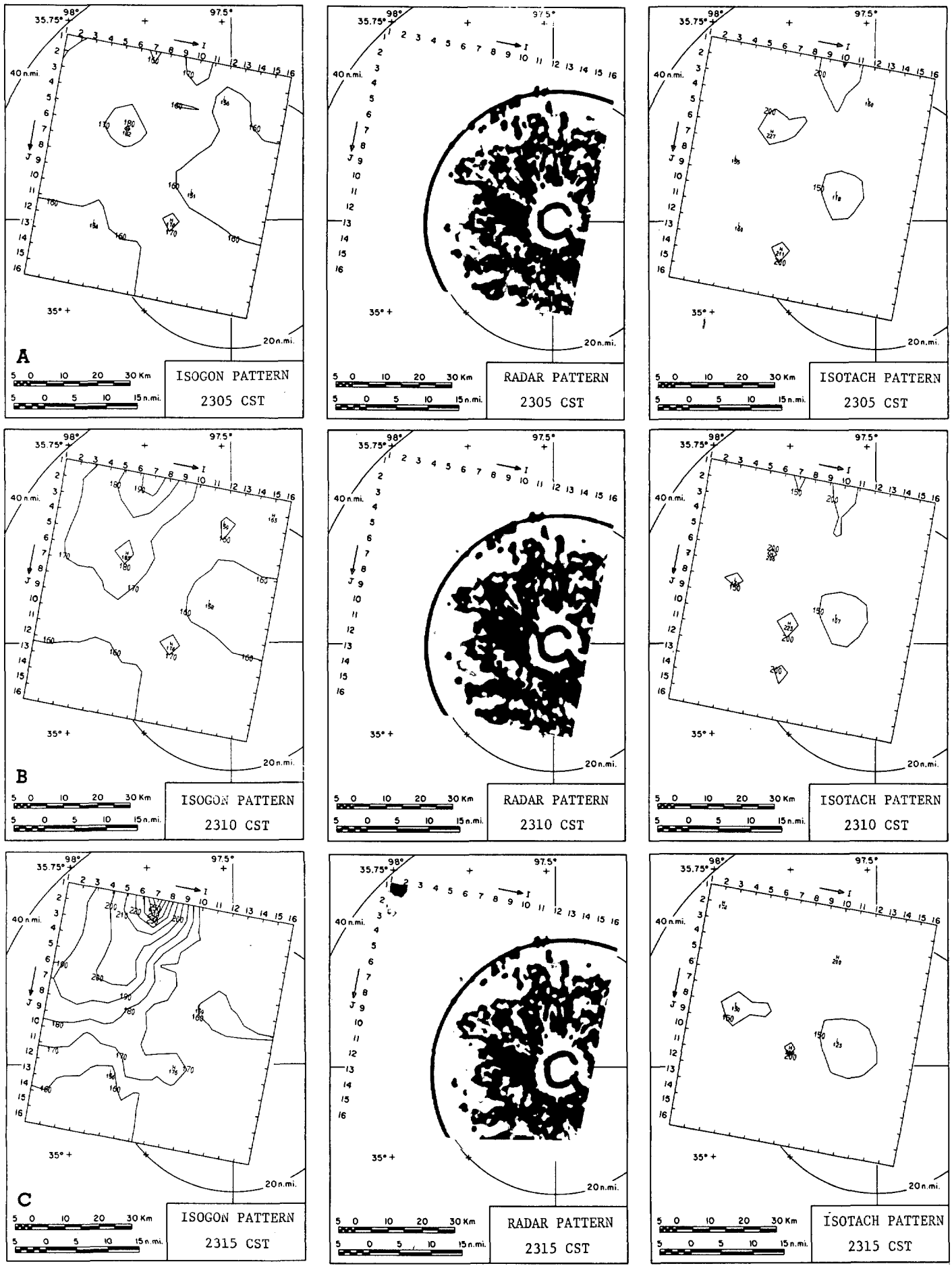

FIGURE 5.—Isogon, radar echo, and isotach patterns in the analysis area on May 31, 1969, at (A) 2305, (B) 2310, (C) 2315, (D) 2320, (E) 2325, (F) 2330, (G) 2335, and (H) 2340 CST.

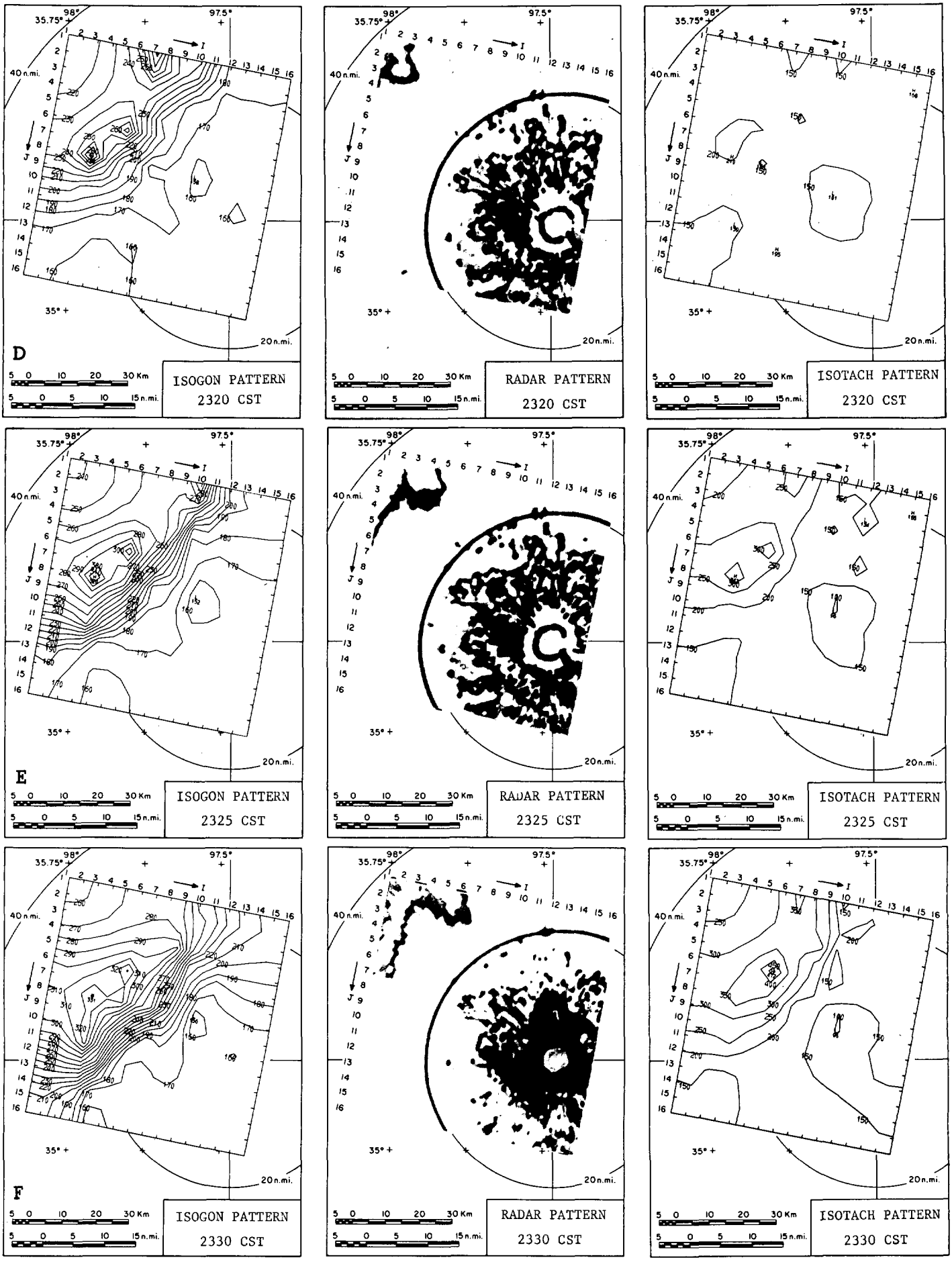

FIGURE 5.—Continued.

408-301 O - 70 - 5

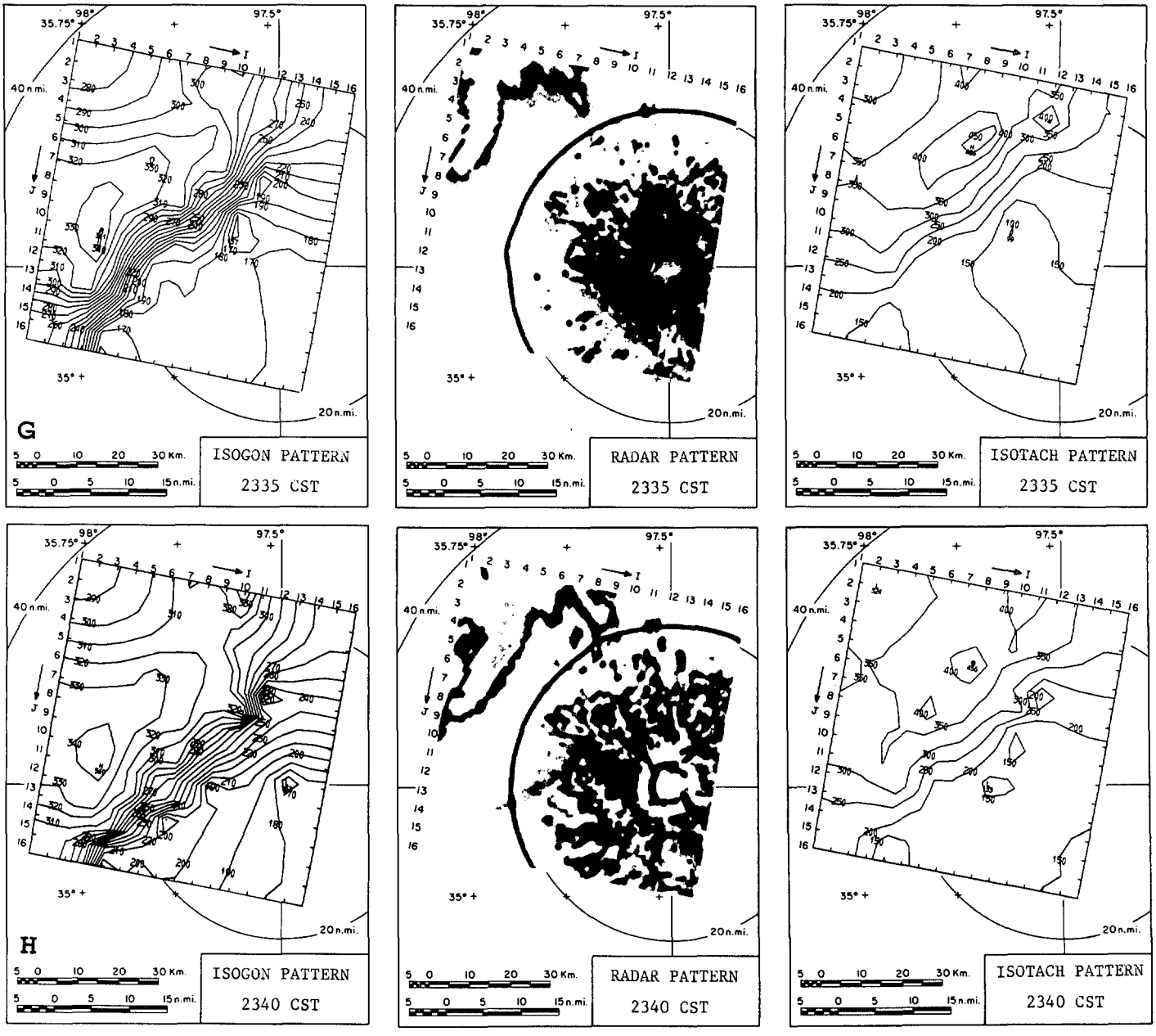

FIGURE 5.—Concluded.

After analyzed values of c_x and c_y are obtained, the isogon and isotach patterns are analyzed separately. First, the wind directions from all stations for the period 2302.5 through 2400 CST are stored at the grid points nearest to each station. Since all data of wind direction indicate that the directions increased monotonically from about 160° to some values less than 360°, the difficulty of non-uniqueness of direction, that is, 10° is equal to 370° for instance, did not appear in the calculation. Normally, calculation by u and v components avoids that multiple-value problem, but this case study was made on the wind direction data for the above reason. The wind direction data were thus used as $\tilde{\varphi}$ in eq (43). The weights $\tilde{\alpha}$, α_t, and α_s are chosen in the same manner as βs. The analyzed isogon patterns φ were displayed on a DD80 cathode-ray representation on the CDC 6600 computer system at the National Center for Atmospheric Research, Boulder, Colo. The patterns thus obtained are for every 2.5 min for the period 2305, 2307.5, 2310, . . . , 2357.5 CST.

Figure 5 shows the isogon, radar echo, and isotach patterns at 5-min intervals between 2305 and 2340 CST. Figure 5A contains the isogon, radar echo, and isotach patterns at 2305 CST. At that time, the radar echo pattern showed the ground echo only. The center of the echo pattern is the NSSL at Norman, Okla.; and the circles shown in the figure are of 20-mi concentric range. No precipitation echo appears in this figure. The isogon pattern (units, degrees) and the isotach pattern (units, $\frac{1}{10}$kt) in figure 5A indicate that a S–SSE wind with a relatively uniform

speed of between 15–20 kt covered the area at 2305 CST. It is interesting to note that relatively higher wind speed areas (say 20 kt or higher) are in positive correlation with the areas of more southerly currents (closer to 180°). Figure 5B shows those at 2310 CST. The storm systems were still outside area ABCD. However, the influence of the storm systems appeared in the wind direction to the west. It is interesting to note that the isotach pattern seems to show no disturbance of the storm systems at that time. An interesting question may be raised as to why the isogon and isotach patterns did not simultaneously reflect the storm systems in their environment. The influence was shown in the isogon pattern earlier than in the isotach pattern. This feature becomes more clearly evident in a comparison of the isogon and isotach patterns in figures 5C and 5D. The storm systems that produced the gust began to appear in the northwest corner of area ABCD at 2315 CST and continued to penetrate into the northern portion of ABCD. The gust shown in the isogon pattern (fig. 5B) at 2310 CST seemed to move to the northeast, and another gust front system was most likely developing at the southern edge of the first gust system, as seen in the isogon and isotach patterns at 2320 CST (fig. 5D).

This second gust front system became a well-defined system at 2325 CST (fig. 5E) as it swept eastward over the west half of the central mesonetwork stations. Also, the first gust system is seen in these patterns as it was moving away from area ABCD. The directions of movement of these two gust systems are apparently different, the first one moving northeastward and the second one eastward, or in the east-southeast direction. At 2330 CST (fig. 5F), the second gust became more intensified, having nearly a northerly wind direction and a wind speed reaching 47 kt at station 3A. (Note that the wind speed is a 5-min running average of wind data read every minute from the wind trace and that the peak wind speed should be considerably higher than 47 kt.) This intensification is primarily due to the intensification of the severe storm system II. However, another severe storm system III was developing to the south of II and was moving toward it. This third system could have some effect on the intensification of the second gust system. It is interesting to note that, in the radar pattern at 2330 CST, one isolated echo, possibly from the second gust front system, is shown as a faint dark spot between stations 4B and 4C, or around the location $I=6\sim7$ and $J=7\sim8$. This dark spot, not shown in the previous figures, became more apparent in the subsequent radar echo patterns at 2335 and 2340 CST. The spot developed into a well-defined line running through stations 4C and 5B (or from the position $I=8$ and $J=8$ to the position $I=5$, $J=11$) at 2335 CST. It then moved to the southeast and is seen in the radar echo pattern at 2340 CST as a dark curved line running from position $I=9$, $J=9$ through $I=5$, $J=13$. The leading edge of the precipitation echo followed this gust from about 15 mi behind. The two are nearly parallel. The gust appearing on the radarscope seems to agree very well, as to their locations and evolutions, with the gust appearing in the isogon and isotach patterns.

10. CONCLUDING REMARKS

The theoretical development of the numerical variational analysis method proposed by the author (1958, 1969*a*, 1969*b*) was extended to a case where empirical rules are used as the subsidiary conditions in the variational formalism. In such a case, the subsidiary conditions are written in a form of approximation. A simple subsidiary condition is that a meteorological system moves approximately with a prespecified velocity. This condition has been used in many weather map analyses as a reliable empirical rule. The condition is also used in this study for the numerical variational analysis of the severe storm gust that swept over the NSSL mesonetwork around midnight of May 31, 1969.

The results of the analysis demonstrate the applicability of the analysis method and reveal some features of the gust. One of the significant features of the gust is that the rapid shift of wind direction appeared before the wind speed changed as the gust approached. The time lag between the appearances of these two parameters is several minutes. Presently, the reason for this nature is not clear. Another interesting feature is that storm system II produced a distinct gust front. However, storm systems I and III seemed not to produce such a distinct gust front although system I passed closely by the network area and system III passed over the network area. This feature brings up the question as to the mechanism in the storm associated with gust production. Also, this study seems to suggest the future possibility of using the same approach in the problem of designing a surface observational network appropriate to the local weather phenomena. Based on this study, it is the author's impression that the 1969 network density seems to be higher than required in some areas while additional stations appear to be needed in the northwest and southeast sections of ABCD. A study is underway to determine the effects on the analysis of removing selected stations from the initial field.

APPENDIX

The question of the uniqueness of solution of the residual eq (34) and (35) relates to the question of whether they can be solved as an initial value problem or as a boundary value problem. Prediction is naturally an initial value problem, and analysis is commonly a boundary value problem. The approach by which one intends to include time variation terms with the analysis will now bring the prediction and analysis close together in the residual equations. In this appendix, we use inductive logic to discuss the uniqueness of solution on the basis of the theory of characteristics (Courant and Hilbert 1962). For convenience, Δt and Δx are taken to be infinitesimal.

Then eq (34) and (35) are written as

$$\tilde{\alpha}(\varphi-\tilde{\varphi})-(\alpha+\alpha_t)\frac{\partial^2\varphi}{\partial t^2}-2\alpha c_x\frac{\partial^2\varphi}{\partial t\partial x}-(\alpha+\alpha_s)c_x^2\frac{\partial^2\varphi}{\partial x^2}-\alpha\frac{\partial c_x}{\partial x}\frac{\partial\varphi}{\partial t}-\alpha c_x\frac{\partial c_x}{\partial x}\frac{\partial\varphi}{\partial x}=0 \quad (48)$$

and

$$\tilde{\beta}(c_x-\tilde{c}_x)-\alpha\frac{\partial\varphi}{\partial x}\frac{\partial\varphi}{\partial t}-\alpha c_x\frac{\partial\varphi}{\partial x}\frac{\partial\varphi}{\partial x}-\beta_t\frac{\partial^2 c_x}{\partial t^2}-\beta_s\frac{\partial^2 c_x}{\partial x^2}=0. \quad (49)$$

Let us assume that a characteristic base curve C_0 does exist and is expressed by $\xi(t,x)=0$. The variables φ and c_x and their first derivatives are defined uniquely along C_0, but the outward derivatives of higher order are not uniquely determined. Transforming (t,x) to (ξ,η), where η is orthogonal to ξ, one can rewrite the derivatives as

$$\frac{\partial\varphi}{\partial t}=\frac{\partial\xi}{\partial t}\frac{\partial\varphi}{\partial\xi}+\frac{\partial\eta}{\partial t}\frac{\partial\varphi}{\partial\eta},$$

$$\frac{\partial^2\varphi}{\partial t^2}=\left(\frac{\partial\xi}{\partial t}\right)^2\frac{\partial^2\varphi}{\partial\xi^2}+2\left(\frac{\partial\xi}{\partial t}\right)\left(\frac{\partial\eta}{\partial t}\right)\frac{\partial^2\varphi}{\partial\xi\partial\eta}+\left(\frac{\partial\eta}{\partial t}\right)^2\frac{\partial^2\varphi}{\partial\eta^2},$$

and

$$\frac{\partial^2\varphi}{\partial t\partial x}=\left(\frac{\partial\xi}{\partial t}\right)\left(\frac{\partial\xi}{\partial x}\right)\frac{\partial^2\varphi}{\partial\xi^2}+\left(\frac{\partial\xi}{\partial t}\right)\left(\frac{\partial\eta}{\partial x}\right)\frac{\partial^2\varphi}{\partial\xi\partial\eta}+\left(\frac{\partial\xi}{\partial x}\right)\left(\frac{\partial\eta}{\partial t}\right)\frac{\partial^2\varphi}{\partial\xi\partial\eta}+\left(\frac{\partial\eta}{\partial t}\right)\left(\frac{\partial\eta}{\partial x}\right)\frac{\partial^2\varphi}{\partial\eta^2}.$$

Also, one can write similar ones for other derivatives. When giving attention to the outward derivatives of the second order, $\partial^2\varphi/\partial\xi^2$ and $\partial^2 c_x/\partial\xi^2$, eq (48) and (49) are

$$-\left[(\alpha+\alpha_t)\left(\frac{\partial\xi}{\partial t}\right)^2+2\alpha c_x\left(\frac{\partial\xi}{\partial t}\right)\left(\frac{\partial\xi}{\partial x}\right)+(\alpha+\alpha_s)c_x^2\left(\frac{\partial\xi}{\partial x}\right)^2\right]\frac{\partial^2\varphi}{\partial\xi^2}=F_1 \quad (50)$$

and

$$-\left[\beta_t\left(\frac{\partial\xi}{\partial t}\right)^2+\beta_s\left(\frac{\partial\xi}{\partial x}\right)^2\right]\frac{\partial^2 c_x}{\partial\xi^2}=F_2 \quad (51)$$

where F_1 and F_2 are functions of variables and their derivatives, other than the outward derivatives of the second order. Therefore, the $\partial^2\varphi/\partial\xi^2$ and $\partial^2 c_x/\partial\xi^2$ are uniquely determined if

$$\Delta=\begin{vmatrix}(\alpha+\alpha_t)\left(\frac{\partial\xi}{\partial t}\right)^2+2\alpha c_x\left(\frac{\partial\xi}{\partial t}\right)\left(\frac{\partial\xi}{\partial x}\right)+(\alpha+\alpha_s)c_x^2\left(\frac{\partial\xi}{\partial x}\right)^2, & 0\\ 0 & \beta_t\left(\frac{\partial\xi}{\partial t}\right)^2+\beta_s\left(\frac{\partial\xi}{\partial x}\right)^2\end{vmatrix}\neq 0 \quad (52)$$

As long as at least one of α_t and α_s and also at least one of β_t and β_s is a nonzero value, the characteristic condition will not be satisfied.

Solution of eq (34) and (35) may be determined uniquely as a boundary value problem if the necessary boundary conditions are given. If this numerical variational method is used for predicting future patterns, it is better to solve the problem as an initial value problem. In that case, α_t and α_s or β_t and β_s or both may be taken to be zero.

ACKNOWLEDGMENTS

This study was supported by the Environmental Science Services Administration under ESSA Research Grants E22-43-70(G) and E19-69(G) and in part from the National Science Foundation under Grant GF-291 under the United States-Japan Cooperative Science Program.

The author is deeply in debt to Mr. Kenneth Wilk for his suggestion of the gust analysis and also to Mrs. Kathryn Gray, both of the National Severe Storms Laboratory. I wish to express my thanks for their assistance in providing partially processed NSSL mesonetwork wind data and also for their valuable suggestions and comments for this study. The author would like to extend his appreciation to Drs. E. Kessler and S. L. Barnes, NSSL, for their encouragement and stimulating discussions and to Messrs. Kit Wagner and J. Charba, The University of Oklahoma, for their assistance on the analysis. Also, appreciation is extended to Mmes. Jan Stone, Marcia Rucker, and Kathy Kajinami for their assistance in preparation of the figures.

Acknowledgment is made to the National Center for Atmospheric Research, sponsored by the National Science Foundation, for use of its Control Data 6600 computer and to the Merrick Computer Center at The University of Oklahoma for use of its IBM 360/40 computer.

REFERENCES

Blackman, R. B., and Tukey, J. W., *The Measurement of Power Spectra*, Dover Publications, Inc., New York, **1958**, 190 pp.

Courant, R., and Hilbert, D., *Methods of Mathematical Physics*, Vol. 1, Interscience Publishers, Inc., New York, **1953**, 561 pp.

Courant, R., and Hilbert, D., *Methods of Mathematical Physics* Vol. 2, Interscience Publishers, Inc., New York, **1962**, 830 pp.

Sasaki, Yoshikazu, "An Objective Analysis Based on the Variational Method," *Journal of the Meteorological Society of Japan*, Ser. 2, Vol. 36, No. 3, June **1958**, pp. 77–88.

Sasaki, Yoshikazu, "Numerical Variational Method of Analysis and Prediction," *Proceedings of the WMO/IUGG Symposium on Numerical Weather Prediction, Tokyo, Japan, November 26–December 4, 1968*, Japan Meteorological Agency, Tokyo, Mar. **1969***a*, pp. VII-25—VII-33.

Sasaki, Yoshikazu, "Proposed Inclusion of Time Variation Terms, Observational and Theoretical, in Numerical Variational Objective Analysis," *Journal of the Meteorological Society of Japan*, Vol. 47, No. 2, Apr. **1969***b*, pp. 115–124.

Sasaki, Yoshikazu, "Some Basic Formalisms in Numerical Variational Analysis," *Monthly Weather Review*, Vol. 98, No. 12, Dec. **1970***a*, pp. 875–883.

Sasaki, Yoshikazu, "Numerical Variational Analysis Formulated Under the Constraints as Determined by Longwave Equations and a Low-Pass Filter," *Monthly Weather Review*, Vol. 98, No. 12, Dec. **1970***b*, pp. 884–899.

Thompson, Philip D., "Reduction of Analysis Error Through Constraints of Dynamical Consistency," *Journal of Applied Meteorology*, Vol. 8, No. 5, Oct. **1969**, pp. 738–742.

[*Received March 6, 1970; revised April 23, 1970*]